Electronic Supplementary Material (ESI) for Journal of Materials Chemistry A.

Electronic Supplementary Information

La_2O_3 Interface Modification of Mesoporous TiO_2 Nanostructures Enabling Highly Efficient Perovskite Solar Cells

Shoyebmohamad F. Shaikh, Hyeok-Chan Kwon, Wooseok Yang, Hyewon Hwang, Hongseuk Lee, Eunsong Lee, Sun Ihl Ma, and Jooho Moon*

Department of Materials Science and Engineering, Yonsei University
Seoul 120-749, Republic of Korea

**Corresponding author, e-mail: jmoon@yonsei.ac.kr, Tel.: +82-2-2123-2855, Fax: +82-2-312-5375.*

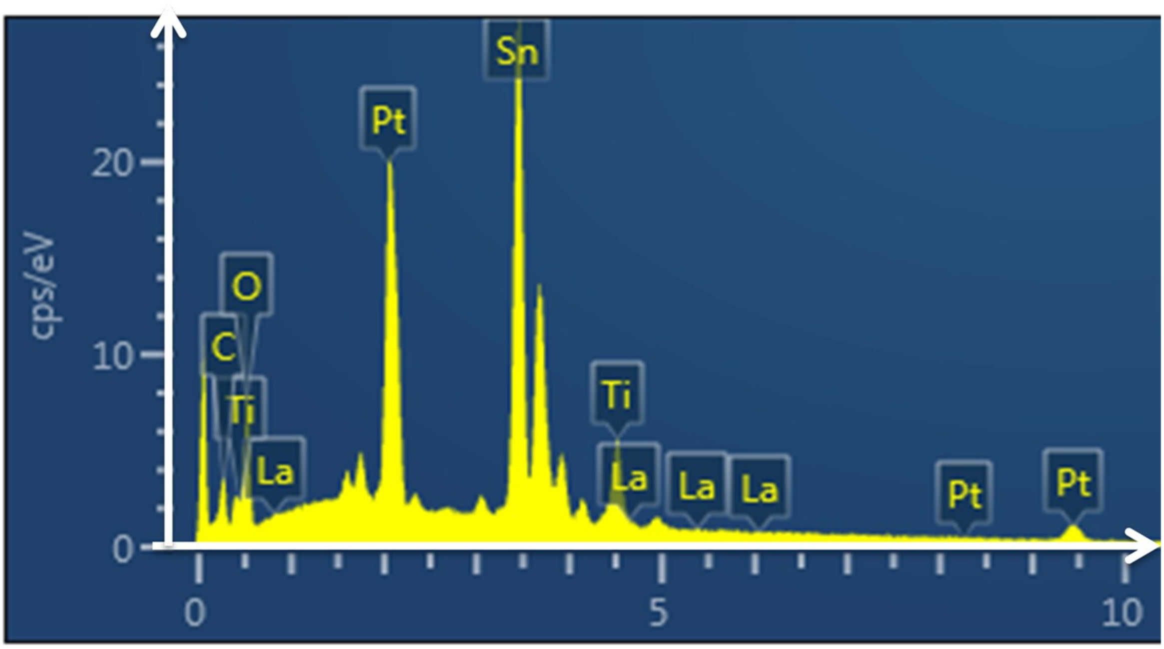

Fig. S1 EDX analysis of an FE-SEM image of mp-TiO_2-La_2O_3 ETL on an FTO substrate.

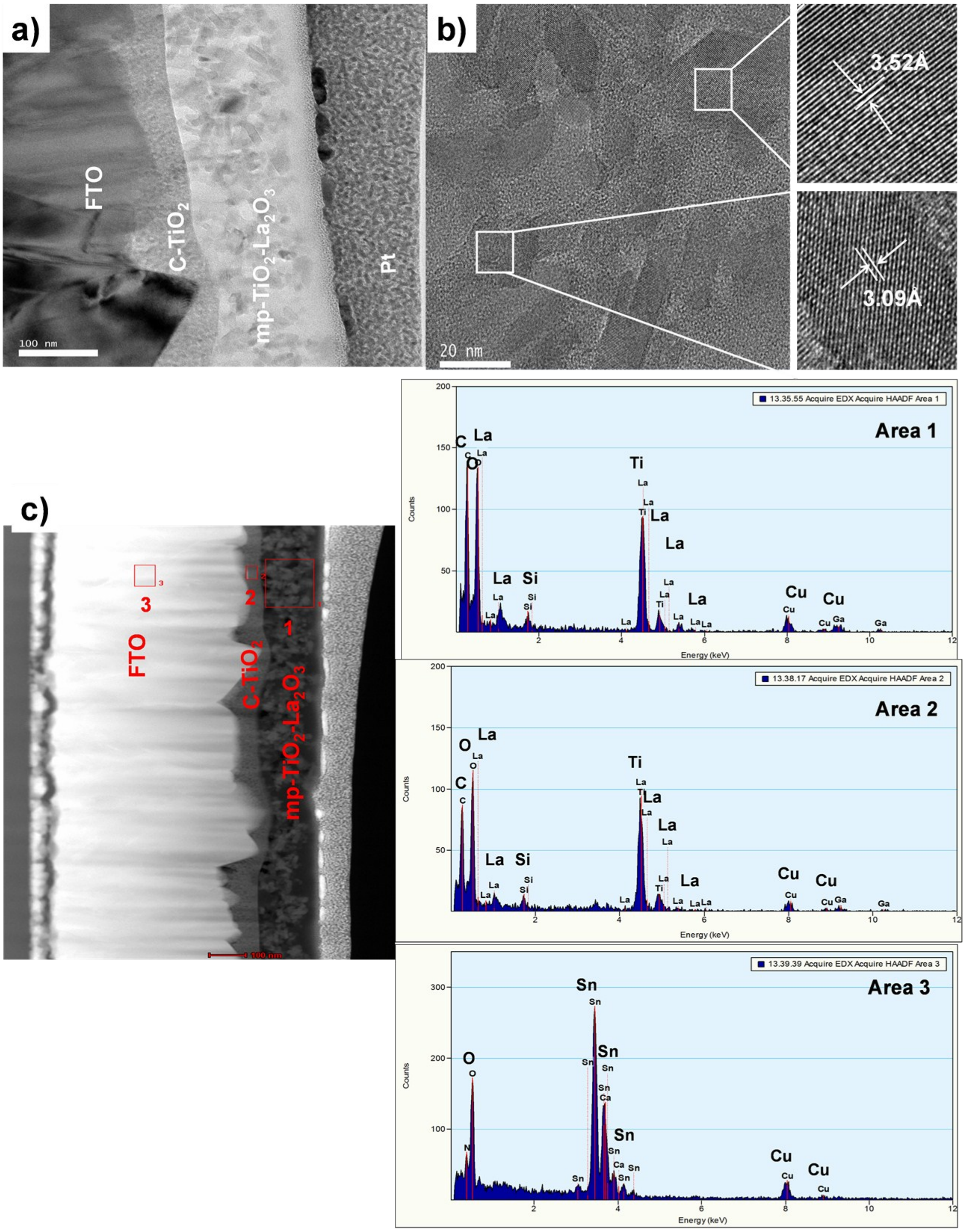

Fig. S2 a) A focused ion beam (FIB) cross-sectioned high resolution transmission electron microscopy (HRTEM) image of mp-TiO_2-La_2O_3, b) high-magnification TEM images of mp-TiO_2-La_2O_3 with *d*-spacing analyses (insets), and c) EDX analysis of FIB cross-sectioned interfaces of FTO/C-TiO_2/mp-TiO_2-La_2O_3 ETLs.

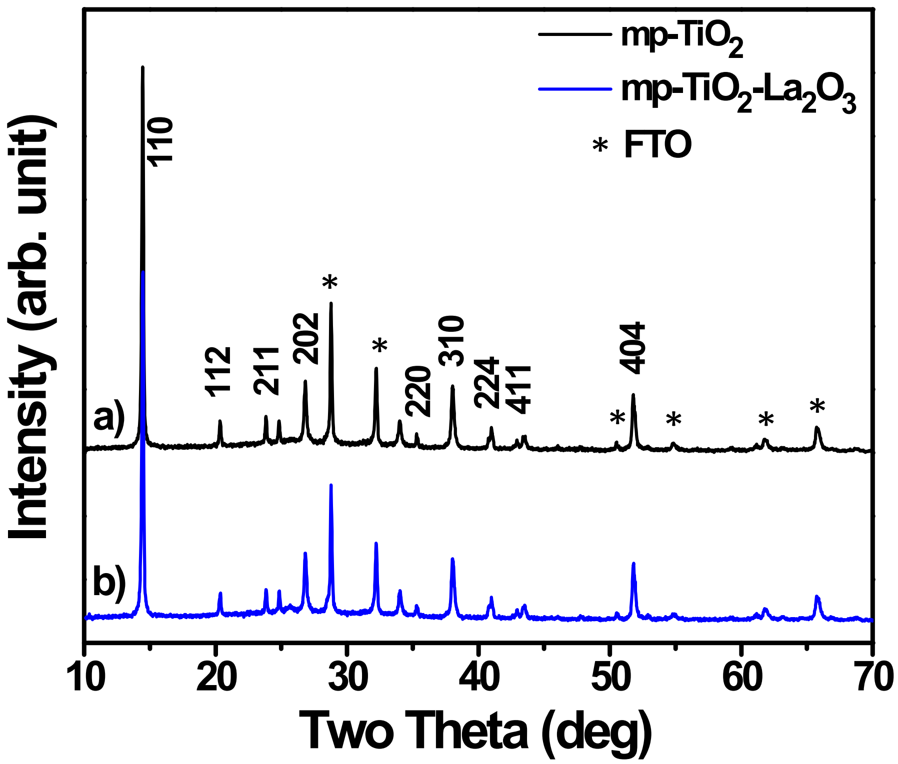

Fig. S3 XRD patterns of (a) mp-TiO_2/$CH_3NH_3PbI_3$ and (b) mp-TiO_2-La_2O_3/$CH_3NH_3PbI_3$. The asterisks (*) indicate FTO substrate peaks.

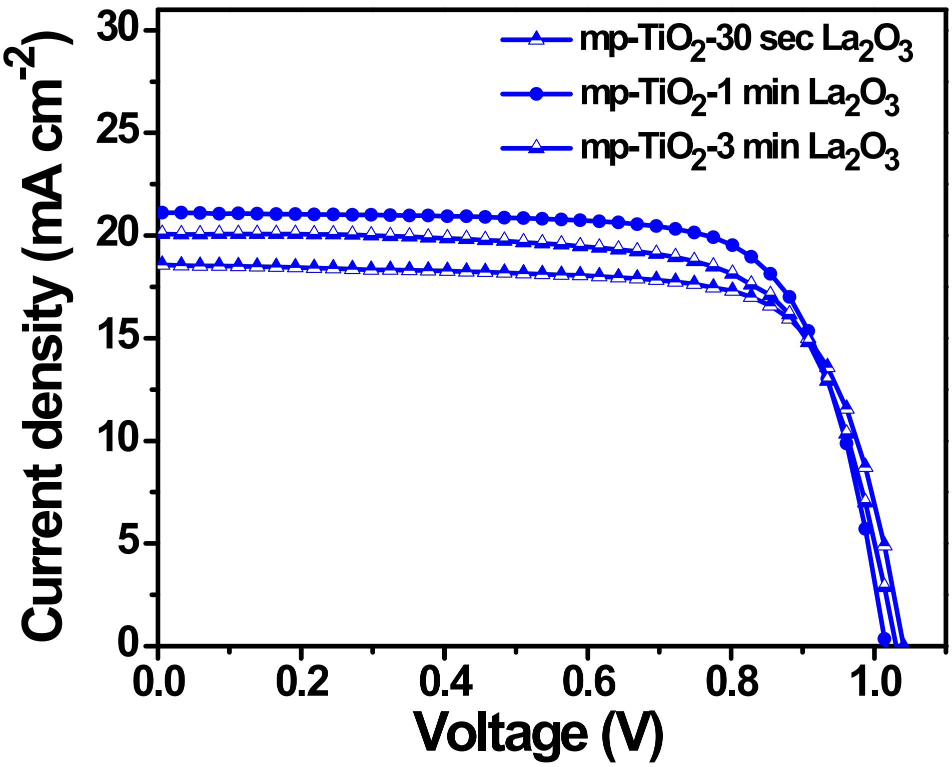

Fig. S4 *J–V* characteristics of an FTO/mp-TiO_2-La_2O_3/$CH_3NH_3PbI_3$/spiro-OMeTAD/gold device under illumination of simulated AM1.5G light (100 mW cm^{-2}). The La_2O_3 interface modification layers were varied using different dip coating times of 30 s, 1 min, and 3 min. The scan rate was constant at 8.6 mV s^{-1} for all the measurements.

Table S1 Summary of photovoltaic performance metrics of the champion devices fabricated by varying the dip coating times

ETL	J_{sc} (mA cm^{-2})	V_{oc} (V)	*FF* (%)	PCE (%)
mp-TiO_2-30 s La_2O_3	18.63	1.00	67.01	12.53
mp-TiO_2-1 min La_2O_3	20.84	1.01	74.64	15.81
mp-TiO_2-3 min La_2O_3	20.36	1.01	70.64	14.55

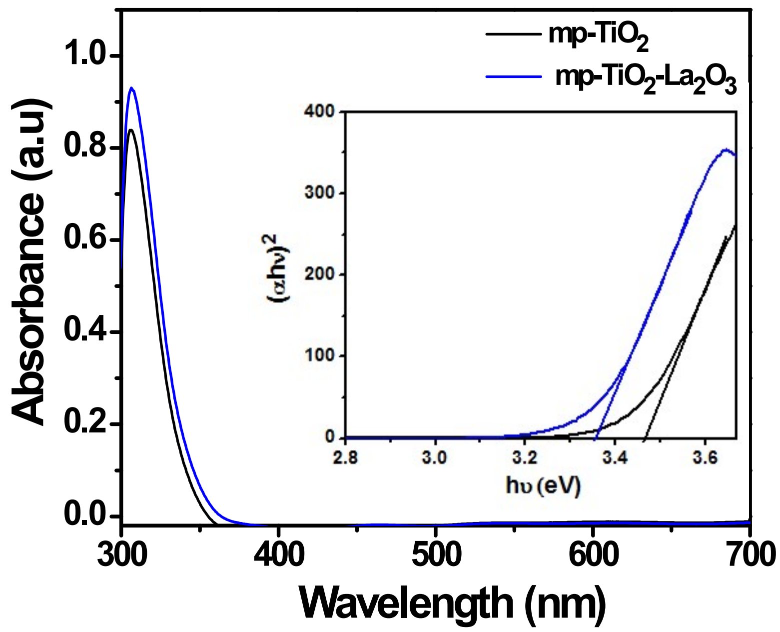

Fig. S5 UV-vis absorbance spectra of mp-TiO_2 and mp-TiO_2-La_2O_3 ETLs before depositing $CH_3NH_3PbI_3$. The inset Tauc plot shows the band gap positions of the mp-TiO_2 and mp-TiO_2-La_2O_3 ETLs.

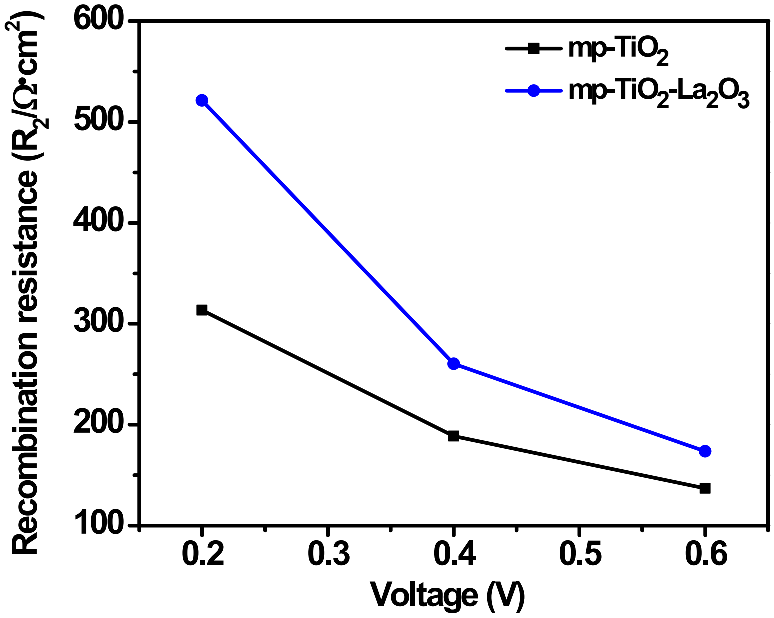

Fig. S6 Recombination resistances of both mp-TiO_2 ETL- and mp-TiO_2-La_2O_3 ETL-based devices obtained at different bias potentials under illumination of 100 mW cm^{-2} AM 1.5.

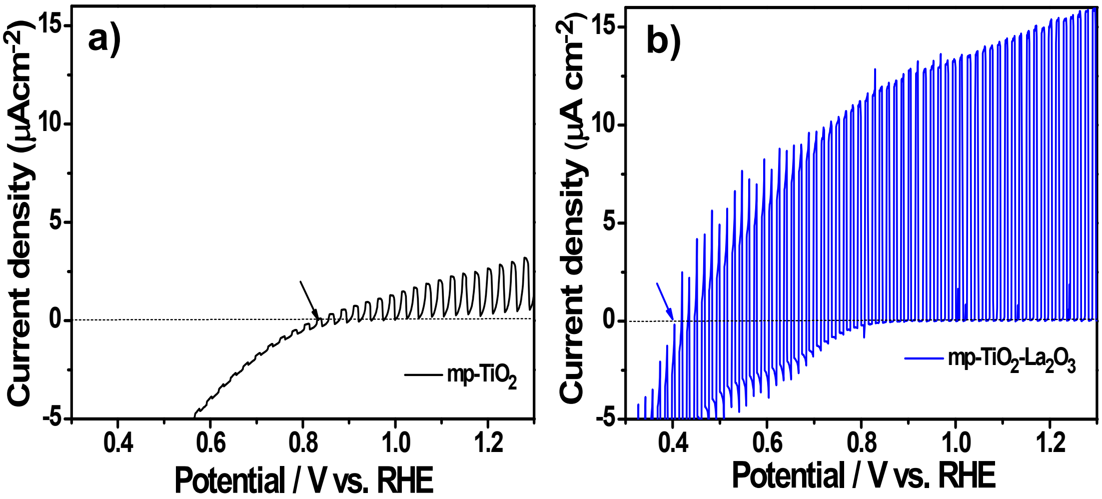

Fig. S7 Photocurrent-potential curve measured in a 0.5 M aqueous Na_2SO_4 solution under illumination of simulated AM1.5 light. The measurement was performed using the three-electrode configuration with a Ag/AgCl electrode as the reference electrode, Pt mesh as the counter electrode, and either (a) FTO/mp-TiO_2 or (b) FTO/mp-TiO_2-La_2O_3 as the working electrode in a 0.5 M aqueous Na_2SO_4 solution.

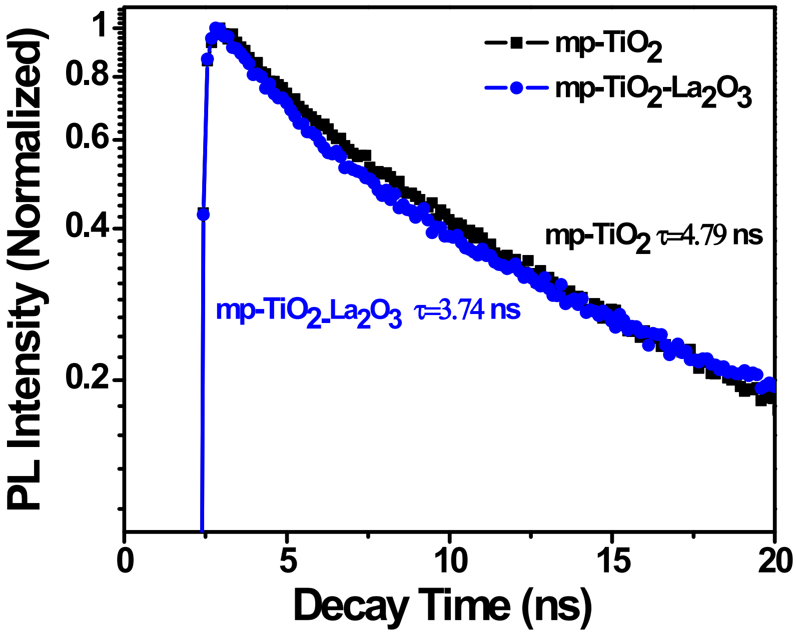

Fig. S8 Time-resolved PL spectra of both ETL samples on a glass substrate including glass/mp-TiO_2/$CH_3NH_3PbI_3$ and glass/mp-TiO_2-La_2O_3/$CH_3NH_3PbI_3$.

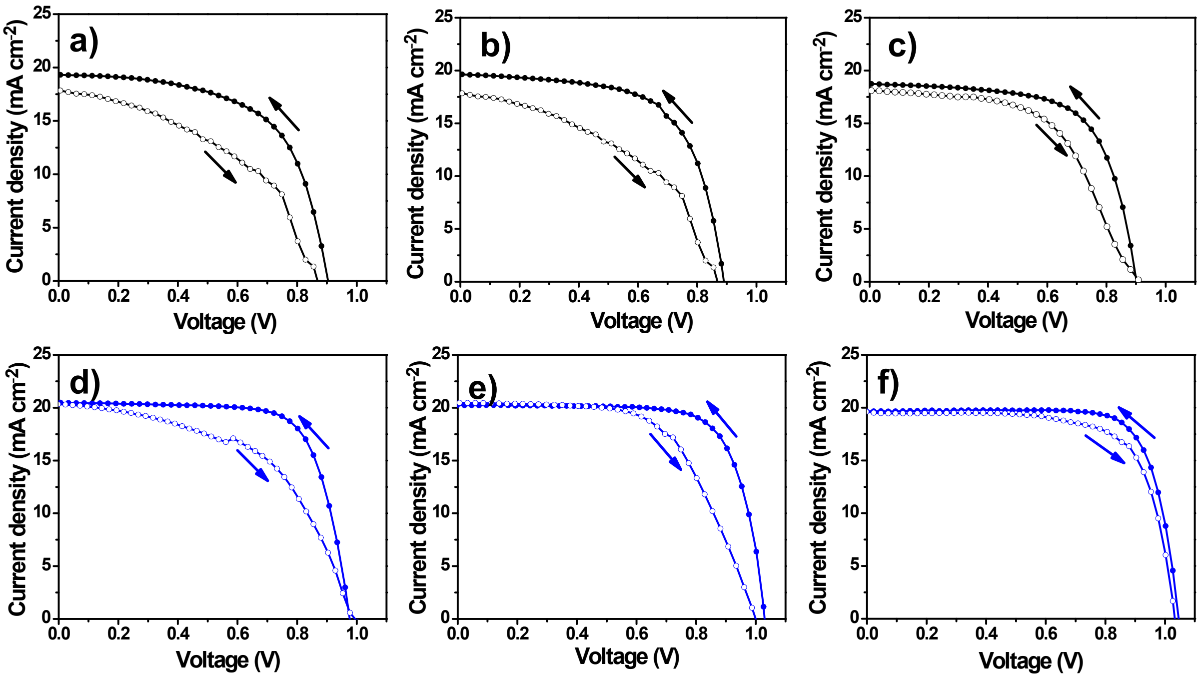

Fig. S9 *J–V* characteristics of forward and reverse scans for both FTO/mp-TiO_2/$CH_3NH_3PbI_3$/spiro-OMeTAD/Au and FTO/mp-TiO_2-La_2O_3/$CH_3NH_3PbI_3$/spiro-OMeTAD/Au devices under illumination of simulated AM1.5G light (100 mW cm^{-2}) at different scan rates of (a, d) 520, (b, e) 52, and (c, f) 8.6 mV s^{-1}.

Table S2 Photovoltaic parameters of both FTO/mp-TiO_2/$CH_3NH_3PbI_3$/spiro-OMeTAD/Au and FTO/mp-TiO_2-La_2O_3/$CH_3NH_3PbI_3$/spiro-OMeTAD/Au devices shown in Fig. S9 (a-f) as a function of scan rate and scan direction

Scan rate (mV s^{-1})	ETLs	Scan direction	J_{sc} (mA cm^{-2})	V_{oc} (V)	*FF* (%)	PCE (%)
520	mp-TiO_2	Reverse	19.28	0.90	60.44	10.53
		Forward	18.20	0.88	39.45	6.53
	mp-TiO_2-La_2O_3	Reverse	20.48	1.00	73.19	15.02
		Forward	20.33	1.04	52.25	10.55
52	mp-TiO_2	Reverse	19.63	0.89	63.42	11.08
		Forward	17.88	0.86	44.32	6.83
	mp-TiO_2-La_2O_3	Reverse	20.21	0.99	74.52	15.48
		Forward	20.44	1.02	59.68	11.87
8.7	mp-TiO_2	Reverse	18.73	0.90	65.73	11.10
		Forward	17.70	0.87	57.83	8.98
	mp-TiO_2-La_2O_3	Reverse	19.65	1.03	77.44	15.81
		Forward	19.63	1.01	70.56	14.38

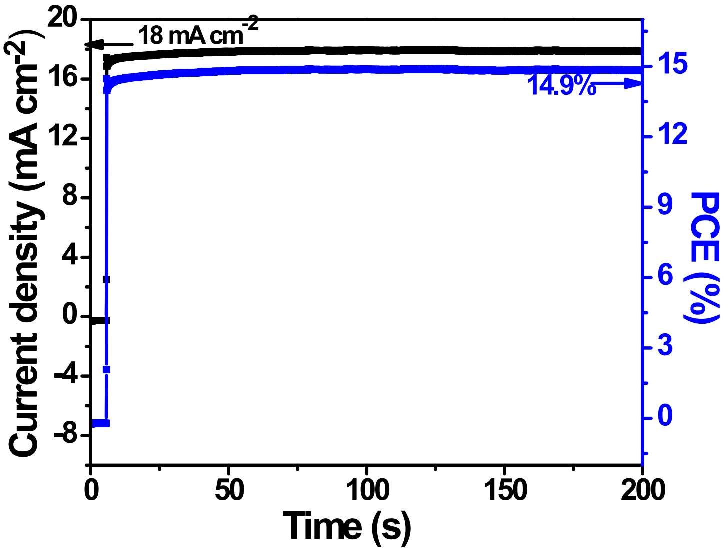

Fig. S10 Stabilized photocurrent density (black) and PCE (blue) measured at the maximum power voltage of 0.83 V for 200 s.

Table S3 Comparative study of interface modifications on TiO_2 ETLs for perovskite solar cell applications

ETL Type and Material	Chemicals/ Method	J_{sc} (mA cm^{-2})	V_{oc} (V)	FF (%)	PCE (%)	Approximate enhancement in PEC (%)	Reference
mp-TiO_2	Cesium carbonate/ Spin coating	19.8	0.97	62.0	11.9	23	[7]
mp-TiO_2-Cs_2CO_3		21.3	1.03	65.0	14.2		
C-TiO_2	Polyoxyethylene/ Spin coating	17.9	1.00	66.0	11.8	20	[10]
C-TiO_2-PEO		20.7	1.02	65.0	13.8		
C-TiO_2	Cesium bromide/ Spin coating	18.7	0.99	69.0	13.1	32	[15]
C-TiO_2-CsBr		20.7	1.06	75.0	16.3		
mp-TiO_2	Magnesium methoxide/ Spin coating	20.11	0.85	67.1	11.4	13	[19]
mp-TiO_2-MgO		20.02	0.89	71.2	12.7		
mp-TiO_2	Aluminum tri-sec-butoxide/ Dip coating	17.6	0.87	67.9	10.4	23	[20]
mp-TiO2-Al_2O_3		20.1	0.96	66.1	12.7		
mp-TiO_2	Lanthanum (III) nitrate/ Dip coating	18.73	0.90	65.73	11.10	46	Present Work
mp-TiO_2-La_2O_3		20.84	1.01	74.64	15.81		